BioMedical Engineering OnLine

RESEARCH

Open Access

Identification of Alzheimer's disease brain networks based on EEG phase synchronization

Jiayi Cao[1,2], Bin Li[3*] and Xiaoou Li[1,2,3*]

*Correspondence:
lib_23@sumhs.edu.cn;
lixo@sumhs.edu.cn

[1] College of Medical Imaging, Shanghai University of Medicine & Health Sciences, Shanghai 201318, China
[2] College of Health Science and Engineering, University of Shanghai for Science and Technology, Shanghai 200093, China
[3] Shanghai Yangpu Mental Health Center, Shanghai 200093, China

Abstract

Objective: Using the phase synchronization of EEG signals, two different phases, PLI and PLV, were used to construct brain network analysis and graph convolutional neural network, respectively, to achieve automatic identification of Alzheimer's disease (AD) and to assist in the early diagnosis of Alzheimer's disease.

Methods: In this paper, we selected outpatients (16 AD subjects, 20 mild cognitive impairment (MCI) subjects and 21 healthy control (HC) subjects) from the outpatient clinic of Yangpu Mental Health Center in Shanghai, China, from January 2023 to December 2023, and collected resting-state EEG data. To collect resting-state EEG data, each patient was asked to sit down with eyes closed for 5 min. Firstly, the acquired EEG data were preprocessed to extract the data in the α-band at 8–13 Hz; secondly, the phase lag index (PLI) and phase-locked value (PLV) were used to construct the brain functional network, and the brain functional connectivity map was visualized by brain functional connectivity analysis. Finally, the constructed PLI and PLV were input into the graph convolutional neural network (GCN) model as node features for training and classification, respectively.

Results: Healthy controls had relatively strong mean brain functional connectivity in the PLV brain network compared to AD and MCI patients. MCI patients showed lower mean brain functional connectivity in the brain network of PLI, while all three groups showed significant differences in brain functional connectivity between parietal and occipital lobes. The GCN model improved classification accuracy by more than 10% compared to using a machine learning classifier. When PLV was used as the nodal feature in the GCN model, the model achieved an average classification accuracy of 77.80% for the three groups of AD, MCI and HC, which was an improvement over the accuracy of choosing raw EEG data and PLI as the nodal feature. The performance of the model was further validated.

Conclusions: The experimental results show that the GCN model can effectively identify the graph structure compared with the traditional machine learning model, the GCN-PLV model can better classify AD patients, and the alpha band is proved to be more suitable for AD resting-state EEG by tenfold cross-validation. The brain network map constructed based on PLI and PLV can further capture the local features of EEG signals and the intrinsic functional relationships between brain regions, and the combination of these two models has certain reference value for the diagnosis of AD patients.

Keywords: Alzheimer's disease, Cognitive impairment, Electroencephalogram, Functional connectivity

Introduction

In this study, in order to solve the difficulty of early AD diagnosis, EEG phase synchronization is used through the combination of brain network and deep learning in order to achieve the purpose of assisted diagnosis. The following is the current status of research at home and abroad of the study: Alzheimer's disease (AD) is a common neurodegenerative disease in the elderly, currently affecting approximately 51.6 million people worldwide [1]. This number is expected to reach 132 million by the middle of the twenty-first century [2]. With a 146.2% increase in mortality in the last decade [3], AD has become a major threat to the life and health of people over 65 years of age. At the same time, the global cost of treatment is $1 trillion and is expected to increase to $2 trillion by 2030 [4]. This imposes a huge overhead on both the patient's family and the national treasury. In its early clinical stages, Alzheimer's disease is referred to as mild cognitive impairment (MCI), progressing to AD, in which patients exhibit symptoms consistent with normal aging. In order to accurately diagnose the MCI stage, histologic analyses of the brain or other complex tests are required, which can be extremely difficult for older patients. Therefore, predicting the transition from MCI to AD is the focus of today's research. Current methods for AD diagnosis include neuropsychological tests, brain imaging, and cerebrospinal fluid examination [5–7]. However, these observations and assessments can be subjective and imprecise and the price of imaging equipment is often expensive. All the above three have limitations in the diagnosis and screening of Alzheimer's disease, while EEG has become a low-cost, non-invasive and usable tool, a real-time recording of the internal brain activity, which is widely used in the diagnosis of mental disorders, and provides a reference and reference for the early diagnosis of Alzheimer's disease [8].

Brain network analysis is a technological advancement in the field of neuroscience that can provide richer information about the functional state of the brain by measuring the connectivity between different regions of the brain [9]. Functional brain networks are complex networks of brain regions that are interconnected and work together to perform different cognitive functions. These networks have been extensively studied in the field of neuroscience. In recent years, with the continuous advancement of technology, researchers can use techniques such as EEG or functional magnetic resonance imaging to study these networks [10]. Some important advances have been made in the study of functional brain networks, such as the discovery of many brain regions with different cognitive functions and that the connections between these regions can predict an individual's behavioral and cognitive performance [11]. Combining EEG and functional brain networks to diagnose AD is a more comprehensive approach, and by analyzing both EEG signals and functional brain networks, researchers can more accurately identify a patient's cognitive function and stage. Phase synchronization in the study of EEG signals can effectively deal with EEG signals affected by changes in synchronization amplitude caused by activities such as eye movements; Handayani et al. [12] found that the brain synchronization of MCI patients was generally lower than that of healthy subjects using phase synchronization analysis. Jalili et al. [13] revealed a specific synchronization by whole-head mapping in the early stages of Alzheimer's disease, which

was characterized by a decrease in phase synchronization in frontotemporal regions and an increase in synchronization in temporal parieto-occipital regions of the left hemisphere. In addition, anterior–posterior cluster phase synchrony was correlated with Mini-Mental State Examination scores, linking cognitive decline in AD patients to regional EEG. Knyazeva et al. [14] showed alterations in functional and effective EEG connectivity between the frontoparietal and frontotemporal lobes. The results suggest that resting-state EEG rhythms reflect abnormalities in cortical neural synchronization and coupling in both prodromal and dominant subjects with AD, possibly reflecting dysfunctional neuroplasticity of neurotransmission in remote cortical networks. Phase synchronization in the study of EEG signals can effectively deal with EEG signals affected by synchronized amplitude changes caused by activities such as eye movements. And the application of phase synchronization principle in brain networks is mainly reflected in the study of brain network connectivity, neural oscillations, and the integration of brain networks during task execution. Through phase synchronization analysis, the functional connectivity and network dynamics between different brain regions can be investigated, which is crucial for understanding how the brain coordinates different regions to support cognitive functions [15]. Zheng et al. [16] analyzed resting-state EEG data from 36 AD patients and 29 healthy controls using time–frequency and band-pass filtered FC metrics. These metrics were estimated by Pearson's correlation, and PLI, and used as input features for support vector machines (SVM). The results showed a significant decrease of functional connectivity in the frontal theta band and a significant increase of functional connectivity in the occipital beta band in AD patients. In addition, a decrease in FC in the central region of the theta band was observed only in AD, and SVM achieved 95% classification accuracy for AD and 86% for HC. Hasoon et al. [17] used PLI on 66 MCI and 25 AD cases to estimate functional connectivity as well as to analyze dominant frequency and relative band power. A network-based statistical toolkit was used to assess differences in network topology. Finally, the classification accuracy of AD by machine learning is 86%. It is clear from the above literature that brain network analysis and phase synchronization have been done separately by researchers. There are fewer studies related to combining the two through deep learning triple classification. In this paper, for the first time, the two studies are combined to triple classify AD, MCI, and HC through phase synchronicity using the GCN model. Based on phase synchronization, it can not only help us understand the exchange and integration of information between different regions of the brain, but also reveal changes in the activity of brain regions when the brain receives instructions. Moreover, phase changes in the oscillatory components of EEG signals at different frequencies can provide information about brain states and disease characteristics, leading to an understanding of the brain's activity patterns and functional connectivity in different states.

In summary, phase synchrony plays a key role in brain networks, which not only helps us to understand the activity patterns and functional connectivity of the brain in different states, but also provides an important tool for us to analyze how the brain coordinates different regions to support cognitive functions. Currently, there are not many studies combining the GCN model with brain networks, so this study innovatively combines the two with phase synchrony. Firstly, functional brain networks were constructed by EEG in terms of PLI and PLV, and the differences in functional connectivity among

the three groups were derived from statistical analysis of the functional connectivity under the same thresholds while locating to the specific electrodes. Secondly, based on the characteristics of graph convolutional neural network, the accuracy of GCN model was compared with machine learning classifiers, respectively; the classification accuracy under using PLI and PLV as well as raw EEG as the node features was compared in GCN model. Finally, tenfold cross-validation is used to verify the performance of the model under different frequency bands. A three-level classification of Alzheimer's disease patients, mild cognitive impairment patients, and healthy controls is achieved, providing a new approach for early assisted diagnosis of AD.

Results

Visual brain network

In this study, functional connectivity matrices constructed based on the above two methods were visualized by using Matlab. The average PLI and PLV matrices of the three groups were used to generate brain network maps. As shown in Fig. 1, Brainnet software was used to map the brain network of the three groups of people based on PLI, from which it can be seen that the threshold range of PLI is between 0.32 and 0.39. Brain connectivity can be found to be generally higher from the AD group, especially in specific brain regions such as the parietal and occipital lobes, which may be related to the pathogenesis of AD. As shown in Fig. 2, Channels with significant PLI variability were extracted, in the comparison among the three groups ($p < 0.05$). As shown in Table 3, At the O1-P3 electrodes, the MCI group had fewer and sparser functional connections compared with the AD and HC groups. This indicated that the strength of functional connectivity was worse in MCI in the same threshold range, while both AD and HC groups were strongly correlated and they had more connections. Specifically, the HC group showed stronger connections between the parietal and occipital lobes. In contrast, the MCI groups exhibited a relative lack of strong connections between these brain regions.

As shown in Fig. 3, Brainnet software was used to map the brain network of the three groups of people based on PLV, from which it can be seen that the threshold range of PLV is between 0.63 and 0.89. Brain connectivity can be found to be generally higher from the HC group, especially in specific brain regions such as the parietal and occipital lobes. As shown in Fig. 4, Channels with significant PLV variability were extracted, when

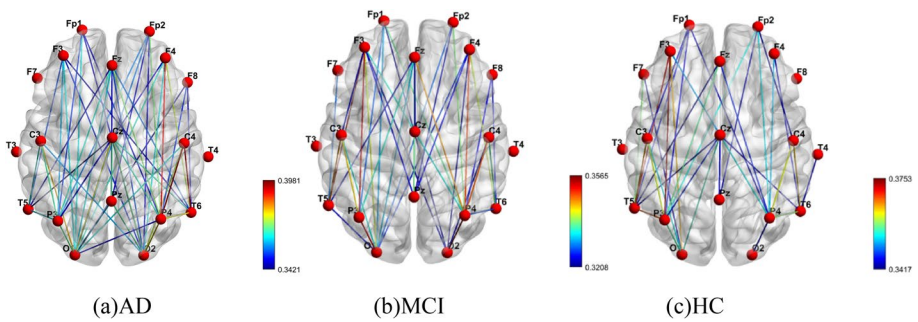

Fig. 1 PLI visual brain network of AD, MCI and HC groups

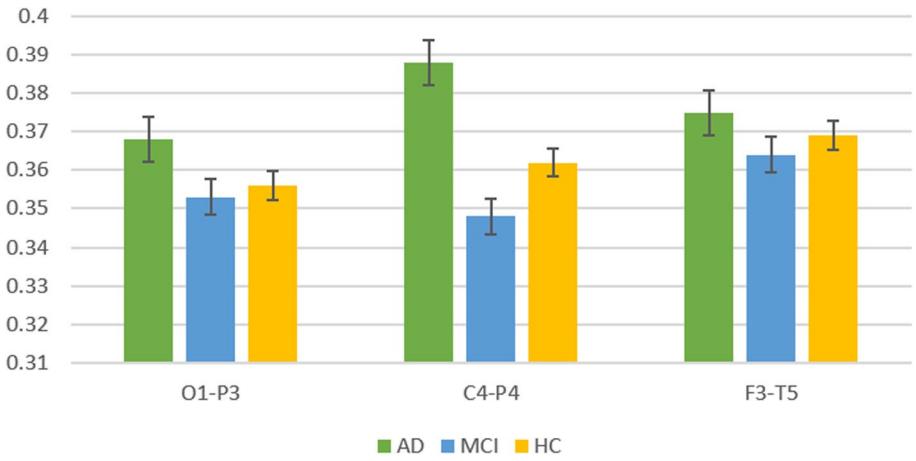

Fig. 2 Channels with significant differences—PLI

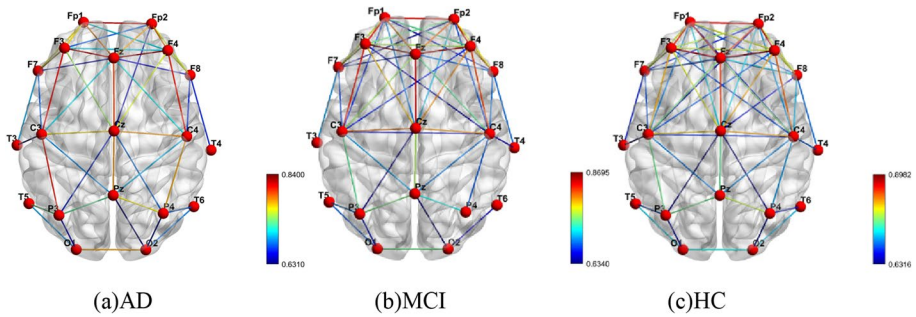

Fig. 3 PLV visual brain network of AD, MCI and HC groups

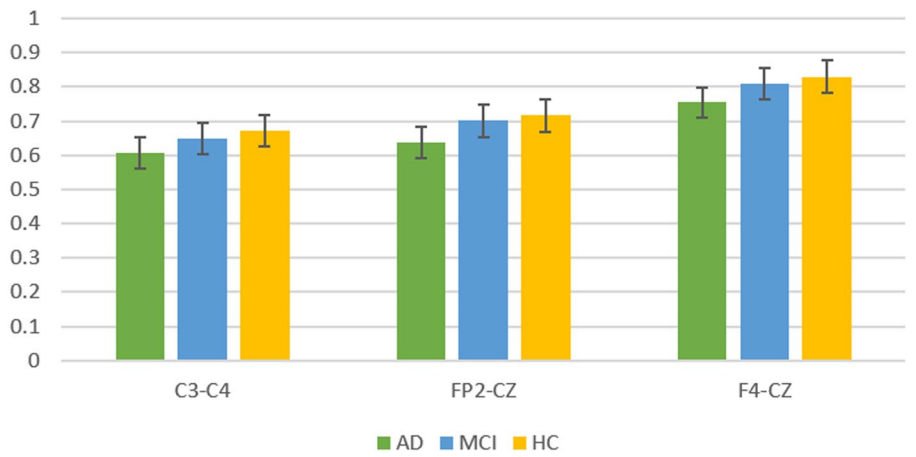

Fig. 4 Channels with significant differences—PLV

comparing the three groups ($p < 0.05$). As shown in Table 5, At the FP2-CZ electrode, the HC group had more and denser functional connectivity compared to the AD and MCI groups. This suggests that in the same threshold range, the functional connectivity of

HC was better in terms of strength, whereas the connectivity of AD and MCI groups was less and all of them were weakly correlated. Specifically, the HC group showed stronger connections between the parietal and frontal lobes. In contrast, the AD group showed a relative lack of connectivity between these brain regions. The MCI and HC groups were closer only in terms of a lack of relatively strong connectivity between brain regions. PLV and PLI brain network analyses were in agreement with the results.

Classification performance

We used the GCN model to categorize and recognize the three groups of AD, MCI and HC, and the framework structure is shown in Fig. 5. In this paper, we divided the dataset into three subsets for training, validation and testing. The ratio of training set, test set, validation set division in the manuscript is 7:3:1. Specifically, 45 instances of data samples were randomly selected and assigned to the training set, while the remaining 12 instances were assigned to the test set. In the training set, a further 5 instances of samples are separated as the validation dataset. This partitioning strategy ensures that the model can be trained on most of the data (40 instances), while also having a separate validation set (5 instances) for monitoring the model performance and performing hyper-parameter tuning during training.

In this paper, we choose three common metrics: accuracy (ACC), sensitivity (SEN), F1-score, recall (REC) to evaluate the model key metrics. Accuracy reflects the ability of the model to correctly judge the overall samples, and the larger its value, the better the performance. Sensitivity reflects the ability of the classifier or model to correctly predict negative samples, the larger the value the better the performance; the same is true for the F1-score. It is defined as follows: $(ACC = (TP + TN)/ (TP + FN + TN + FP)$, $SEN = TP/ (TP + FN)$, $F1\text{-score} = (2 \times SEN \times REC)/ (SEN + REC)$, and $REC = TP/ (TP + FP)$ where TP, TN, FP, and FN are true positive, true negative, false positive, and false negative, respectively. Since EEG is a non-stationary random signal with low signal-to-noise ratio, and the use of different features can significantly affect the classification results. In this paper, we explore the changes in the results of brain networks for its classification under different phases. The raw EEG is added to the model as a comparison, raw EEG is here the pre-processed EEG. The results are shown in Table 1. When the original EEG signal is selected as the node feature, the classification accuracy of the GCN model is 72.00%, the sensitivity 69.70%, the F1-score 68.50%, and the recall 65.12%; when the PLI is

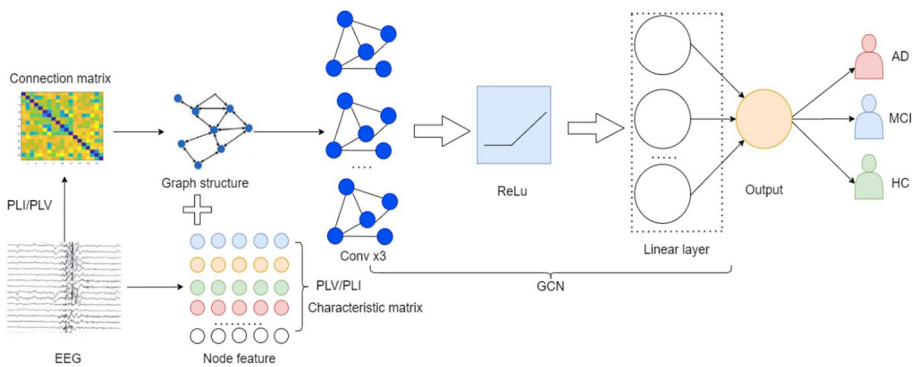

Fig. 5 Structure diagram of convolutional network model applicable to three classifications

Table 1 Experimental results of the GCN model

Model	ACC	SEN	REC	F1-score
GCN-EEG	72.00%	69.70%	65.12%	68.50%
GCN-PLI	74.43%	70.67%	63.88%	72.78%
GCN-PLV	77.80%	73.43%	70.40%	74.64%

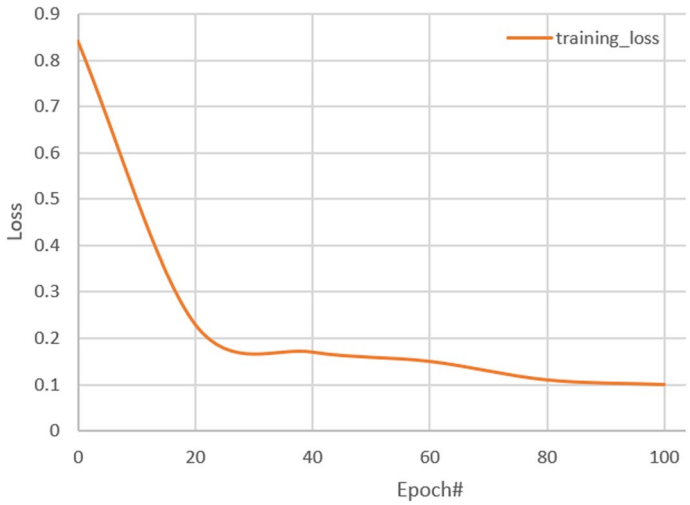

Fig. 6 GCN training loss function

selected as the node feature, the classification accuracy of the GCN model is 74.43%, the sensitivity 70.67%, the F1-score 72.78%, and the recall 63.88%; when the PLV is selected as the node feature, the classification accuracy is 77.80%, sensitivity 73.43%, F1-score 74.64% and the recall 70.40%. It can be seen that the classification accuracy is highest when PLV is selected as the node feature, which further indicates that the selection of node features under the graph structure with phase synchronization has a significant impact on the network model accuracy.

The training loss for datasets is shown in Fig. 6. The training loss initially decreases rapidly, indicating that the model is effectively learning from the training data. After a certain number of iterations, the training loss plateaus, indicating that the model has reached a point of saturation.

Finally, we compare the classification accuracy of the GCN model with other machine learning models, and the results are shown in Fig. 7. From the figure, we can conclude that the classification accuracy, specificity, F1-score and recall of AD and MCI patients and healthy people under the GCN model are 77.80%, 73.43%, 70.40%, and 74.64%, respectively, which is more than 10% higher than that of the GCN model compared to classifying them with machine learning classifiers, respectively. It shows that the graph structure can better distinguish between phase-synchronous brain networks and better classify the three groups of people.

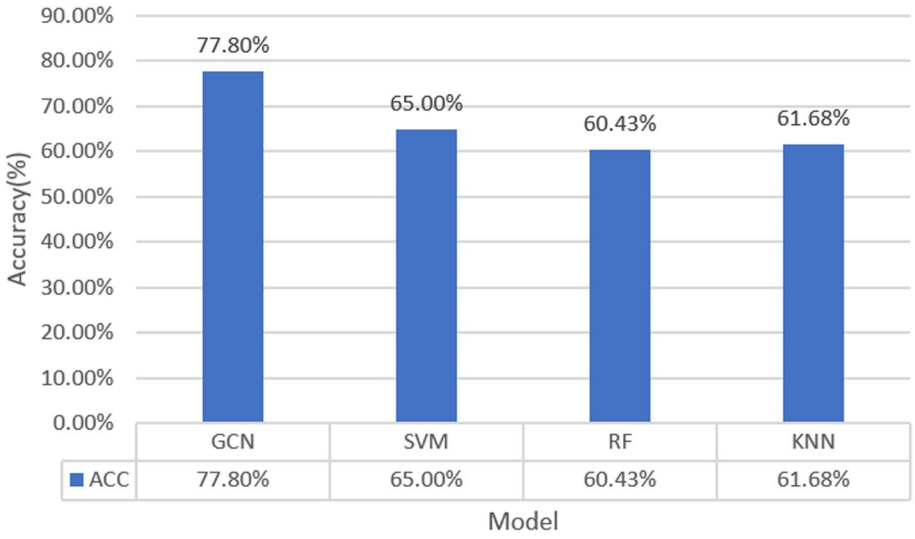

Fig. 7 Comparison of GCN and machine learning classification accuracy

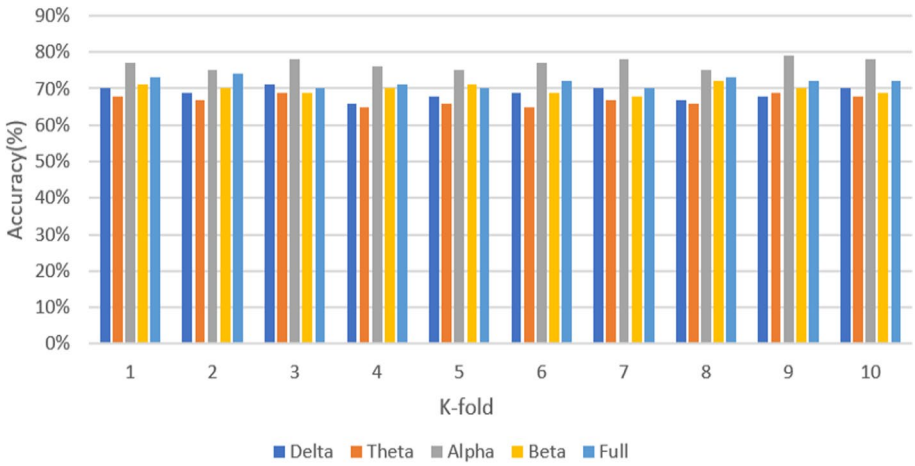

Fig. 8 Tenfold cross-validation plots in different frequency bands

Cross-validation model evaluation

In order to validate the performance of the model and at the same time reduce the influence of chance error and experimental error on the results, this study conducted a tenfold cross-validation and confusion matrix to evaluate the model. In this paper, tenfold cross-validation was first selected to analyze the stability of the model. In order to better understand the properties of EEG signals in different frequency bands, we further subdivided the preprocessed EEG signals into four sub-bands, namely, Delta (0.5-4Hz), Theta (4-8Hz), Alpha (8-13Hz) and Beta (13-30Hz). The whole dataset was randomly divided into 10 copies, 9 copies were used in the training phase of each model and the rest were used for testing. Each band represents the activity of EEG signals at different frequencies, which is an important reference for the diagnosis of AD. In order to visualize the performance of the model on each band, as shown in Fig. 8, the EEG signals are frequency-divided by a Butterworth filter after each segmentation of the dataset, and

the training tests are performed separately while keeping the parameters of the model unchanged. From the figure, it can be seen that, among them, Alpha has the best performance in the sub-band, with an average classification accuracy of 76.80%, which proves that the Alpha band is the best for distinguishing the AD in the resting state. This is consistent with the GCN model classification above.

Secondly, the confusion matrix is used to evaluate the model performance. The final results consisted of the number of correct predictions, with 0 indicating AD, 1 indicating MCI, and 2 indicating HC. Due to the fact that the EEG of 2 MCI patients was not able to reach the signal quality required for use even after pre-processing, only 18 MCI patients were used here, participating in the evaluation of the confusion matrix. The results showed that 16 cases of AD, 18 cases of MCI, and 21 cases of HC were used in the confusion matrix. It is clear from the classification of AD that of the 16 cases of the patients, 12 patients were correctly classified, 3 cases were predicted as MCI, and 1 was predicted to be HC. From the classification of HC it is clear that of the 21 cases, 19 patients were correctly classified, 1 patient was predicted to be MCI, and 1 patient was predicted to be HC. Since only 18 patients with MCI were used, of the 18 patients, 14 patients were correctly classified, 3 patients were predicted to be AD, and 1 patient was predicted to be HC. So the confusion matrix correctly classified with the number of people remained consistent. The model confusion matrix is shown in Fig. 9. Due to the uneven proportions of AD, MCI, and HC subjects in the sample, which may have had some impact on the results, although there were a certain number of outliers for each indicator, the results of multiple runs of the model performed excellently, and the model runs yielded high levels of realism in the results.

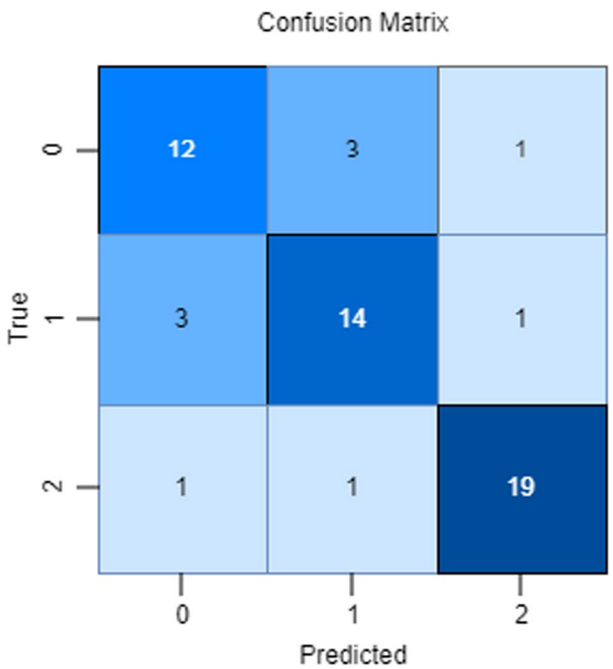

Fig. 9 The confusion matrix obtained in the GCN model

Discussion

In this study, we investigated the effects of brain network features under phase synchronization on the classification of cognitive impairment in three groups of people based on resting-state EEG data. Firstly, the EEG data were preprocessed to obtain purer EEG data. Secondly, the neighborhood matrix was obtained by calculating based on the phase features PLI and PLV, and the brain network was constructed, and through statistical analysis we found that the brain networks of the three groups differed significantly in the memory function of specific brain regions, and this brain network variability was significantly correlated with the reduction of cognitive function. In PLV, the average brain function connectivity was stronger in HC group. In PLI, the MCI group exhibited lower mean brain functional connectivity. And the differences in brain functional connectivity among the three groups were mainly between the parietal and occipital lobes. Brain networks can be mined for cognitive memory features from the information flow, topology, and local features of the orientated brain network [18], reflecting both the connectivity relationship between nodes and the degree of interaction between nodes [19], so as to explore the effects of different populations on brain networks under resting tasks for the difference analysis of AD, MCI, and HC brain networks [14]. Last, the brain network performance of the three populations was classified and evaluated using GCN, which unlike previous studies, classified AD, MCI, and HC into three sets of classes, and the GCN model increased the triple classification accuracy by more than 10% compared to using machine learning classifiers. Meanwhile, the original data, PLI and PLV were used as inputs for the node features of the model, respectively, and when PLV was used as a node feature in the GCN model, the model achieved an average classification accuracy of 77.80% for the triple groups of AD, MCI and HC, which was an improvement over the accuracy of choosing the original EEG data and PLI as node features. Finally, ten-fold cross-validation was performed on different frequency bands, respectively, and the results showed that the accuracy rate of α-band was the highest. The performance of the model was further validated. It shows that our research programme is feasible.

Some of the early relevant studies are listed below: Khazaee et al. [20] performed multivariate Granger causality analysis by using machine learning on resting-state data from 34 cases of AD, 89 cases of MCI, and 45 cases of HC to calculate each directed graph measure. A classification accuracy of 73.3% was achieved for AD, MCI and HC using optimal features and Bayesian classifier Parisot et al. [21]. In this paper, we present a comprehensive evaluation of a generalized framework that can be used for brain analysis of large populations. The framework utilizes graph convolutional networks, and represents the population as a sparse graph where its nodes are associated with imaging-based feature vectors and phenotypic information is pooled into edge weights. The performance of the framework was tested on two large datasets (ABIDE and ADNI) with different underlying data, and the classification accuracies on ABIDE and ADNI were 70.4% and 80.0%, respectively. Recent studies have shown that: Zhang et al. [22] calculated EEG power spectra, spectral entropy, and phase synchronization index characteristics of left/right frontal, temporal, central, and occipital brain regions by using two groups. In most of the brain regions, significant differences were found in the AD group compared to the NC group. Zhou et al. [23] classified AD as a graph classification task using brain point data. Second, a local attention layer is

designed to capture and aggregate the interaction information between node neighbors. And a global attention layer is introduced to capture the contribution of each node to the graph representation. Compared with the classical models, the experimental results show that our model outperforms six classical models. Sun et al. [24] human study utilized EEG signals, genotypes and polygenic risk scores as features of machine learning models. Statistical analysis showed significant correlation between EEG signals and clinical presentation. Puri et al. [25] study proposed a new bi-orthogonal wavelet filter bank for decomposing EEG signals from HC subjects, MCI and AD patients into desired EEG signal bands. New design methods are proposed to reduce the complexity of current dual orthogonal wavelet filter banks. Three different features are computed from each EEG signal sub-band to obtain higher accuracy. This is consistent with the findings of previous studies [26–31]. It can be seen from the early studies and the current stage that the early researchers usually use machine learning and simple GCN models for classification, while the current stage researchers pay more attention to mining relevant features from patients' brain regions, so as to better localize the specific brain regions for classification.

However, this paper still has limitations: firstly, the sample size is small; only 16 patients with AD, 20 patients with MCI and 21 healthy controls were collected in this paper, totalling 57 cases. In the future, the sample data will continue to expand, and controlled experiments will add credibility. The second is the lack of generalizability. In this paper, PLI/PLV in the same step was chosen as the differentiation criterion between AD and MCI, but due to the large scope of the same step. Its generalizability needs to be verified in more aspects. Subsequently, it will continue to dig deeper into the weighting properties in the phase synchronization characteristics and incorporate the model to obtain better results which are applicable to a wide range of generalization.

Now, some researchers are combining several indicators: Roster et al. [32] Connections between brain regions form a matrix of connections (MC). To construct the MC, different metrics such as Granger causality test, Pearson correlation and Spearman correlation metrics were used to quantify the strength of connections between two brain regions. Then, the generated MC was put into a convolutional neural network for EEG signal classification. You et al. [33] utilized the sequence features of EEG and human gait features to classify AD, MCI, and HC with a classification accuracy of 91.70%. This attention-based spatio-temporal graph convolutional network can automatically extract the features of EEG and gait data, which reduces human intervention and achieves better classification results. Mammone et al. [34] extracted the power spectral density features of EEG from 63 patients with AD, 63 patients with MCI, and 63 healthy controls and classified them by convolutional neural network, and the results showed that the accuracy of the triple classification was up to 83.3%, which led to the conclusion that the power spectral density can also be used as a data to characterize the information of cognitive impairment.

The quantification of study metrics by the above researchers in conjunction with the characteristics of clinical features provides us with innovative ideas for the future. In this paper, AD, MCI and HC were effectively identified by combining phase features. It is important to note that our own small amount of data and discrepancies

between data still have their limitations. Secondly, the EEG in this paper only used the resting state, and lacked the task-state experimental paradigm for further comparison. In the future, we will continue to increase the amount of data, explore new task-state paradigms, combine the clinical scale features of the three groups, enrich the interpretability by multimodal fusion, and adjust the model parameters to include the attention mechanism, in order to achieve higher classification accuracy and better assist in the diagnosis of Alzheimer's disease.

Conclusion

In this study, we performed brain network analysis on resting-state EEG data of AD patients, MCI patients and healthy controls. Two different phases based on PLI and PLV in the alpha frequency band were extracted to construct brain functional connectivity maps, and the functional connectivity analysis study revealed that the different functional connectivity variability among parietal, frontal, and occipital lobes in the AD, MCI, and HC groups in the resting state in the three populations indicated that there were different degrees of differences and impairments in this brain region. Meanwhile, we proposed a graph convolutional neural network classification model incorporating phase synchronization, when PLI is used as the connectivity matrix and PLV is used as the node features, and verified the good performance of the model cross-validation and using confusion matrix on our own dataset. The experimental results show that the GCN model can effectively identify AD patients and achieve automatic classification of cognitively impaired patients, and it is better than the traditional machine learning model GCN. The alpha band has the highest accuracy in cross-validation, proving that the alpha band is more suitable for the resting-state experimental paradigm. The method proposed in this study has potential applications as an AD aid diagnostic tool in the clinical setting, and with future improvements, it is expected to be a new means of clinical diagnosis of AD, with great promise for clinical applications.

Materials and methods

Research design

The research process of brain functional network analysis usually includes 3 parts: collecting data, constructing brain functional networks and analyzing network properties. The overall process of this study is shown in Fig. 10. Firstly, the EEG signals are preprocessed to obtain pure signals. Second, the frequency domain features of the EEG signals were extracted, and the connection matrix was constructed based on the

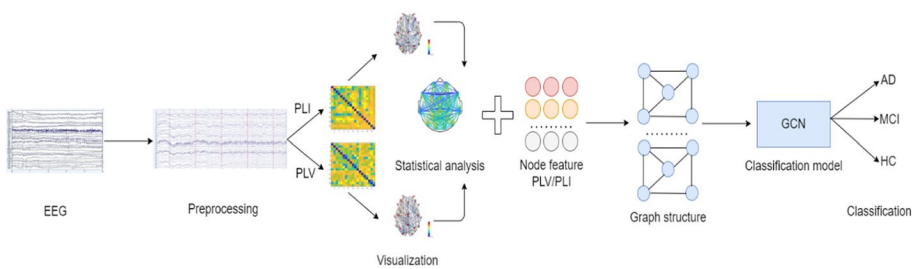

Fig. 10 Overall flowchart

Table 2 Demographic and clinical information of the studied subjects from dataset

Diagnosis	Number	Age	Education	MMSE	MoCA	CDR
AD	16	77.5 ± 8.9	11.1 ± 3.6	20.5 ± 2.5	17.1 ± 3.2	0.8 ± 0.8
MCI	20	70.1 ± 7.0	11.3 ± 3.8	26.9 ± 1.8	21.7 ± 3.4	0.4 ± 0.1
HC	21	71.1 ± 6.7	12.2 ± 4.1	28.0 ± 2.0	24.9 ± 2.9	0.1 ± 0.0

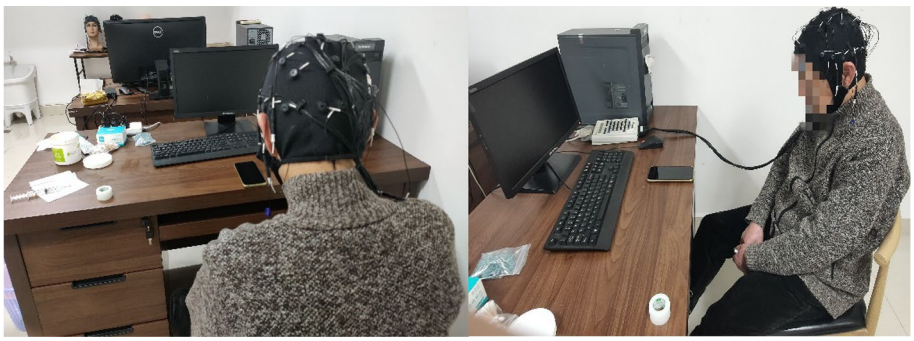

Fig. 11 Schematic diagram of resting-state paradigm

phase synchronization using both the phase lag index and the phase-locked value. Subsequently, the brain network maps of three groups of people under the two methods were constructed by the connection matrix, and the brain network maps were visualized and the brain area variability was analyzed by comparison with the statistical analysis of functional connectivity. Finally, PLV/PLI were added to GCN as node features for classification assessment, respectively, while comparing machine learning classifiers, using tenfold cross-validation and confusion matrix under different frequency bands to assess the model.

Participants

This study was ethically reviewed by the Yangpu Mental Health Center. In this study, three groups of participants were evaluated for AD, MCI and HC as shown in Table 2. Participants were recruited from outpatients of Yangpu Mental Health Center and community centers in Shanghai. At the same time, an informed consent form is signed with the patient. Inclusion criteria: Han Chinese, age 60 years or older, meeting ICD-10 diagnostic criteria, no history of alcoholism, cerebrovascular disease, traumatic brain injury, intracranial tumors, intracranial infections, epilepsy, or other serious mental illnesses. Exclusion criteria: those who were unable to cooperate and complete the examination, exclusion of other mental disorders, somatic diseases, and memory disorders due to substance abuse, and a GDS score > 4. At least 8th grade education and fluent speech. Those who met the criteria were statistically evaluated by specialized physicians on neuropsychological test scales, including the Mini-Mental State Examination (MMSE), Montreal Cognitive Assessment (MoCA), Clinical Dementia Rating Clinical Dementia Rating (CDR). Specialized psychiatrists diagnosed AD according to the diagnostic criteria of the scales and assessed the severity of AD symptoms using the scales, which were recorded in a quiet, closed room.

Experimental paradigm

We used Eprime 2.0 software for experimental design and editing, and designed a resting-state EEG acquisition method as shown in Fig. 11. Each patient needs to be seated with eyes closed for 5 min, during which no speech, fidgeting, falling asleep and other behaviors are allowed, and repeated twice to take the best EEG recording state. The EEG signals were recorded with a NeuroScan SynAmps2 amplifier at a sampling rate of 1000 Hz, and the impedance of each electrode was kept below 10 kΩ, and the electrodes were placed on the scalp according to the international 10–20 system. All experimental data were recorded in a quiet, closed room with no bright light and moderate temperature and humidity. Before participating in the experiment, all participants read and signed the informed consent form.

EEG data set

The data used in this study were collected by myself at the Shanghai Yangpu Mental Health Center, and the dataset consisted of EEGs from 57 subjects, including 16 AD subjects, 20 MCI subjects, and 21 HC subjects. Since human cognitive abilities naturally deteriorate with age [35], this study ensured that the age of AD and MCI and HC subjects needed to be greater than 60 years old to exclude the effect of age on the classification results. In addition, this study considered the effect of subject gender, but a two-sided test proved that gender differences were not statistically significant in relation to clinical status [36]. Subject details are shown in Table 1. Nineteen electrode positions (Fp1, Fp2, F7, F3, Fz, F4, F8, T3, C3, Cz, C4, T4, T5, P3, Pz, P4, T6, O1, and O2) were selected on the scalp according to the international 10–20 system, and the closed-eye resting-state EEG was acquired for 300s using earlobe electrode landmark unipolar connections with a sampling frequency of 1000 Hz.

In order to minimize the artifacts, the EEG signals were preprocessed. First, the EEGLAB toolbox in Matlab was used to band-pass filter the 19-channel EEG signals from 0.1 to 30 Hz. When performing high pass filtering in EEGLAB, we set the lower threshold frequency of 0.1Hz, and the components below the frequency will be filtered out. For low-pass filtering, we set an upper limit frequency of 30 Hz. Finally, trap filtering is used to eliminate frequency-specific interference, which can accurately remove fixed-frequency noise and improve the purity of the signal. After all the filtering is done, we check the data of each channel to make sure that the high and low frequency noise has been effectively removed. Next, artifacts in the EEG signals were removed using the independent principal component analysis (ICA) method in the EEGLAB toolbox, where ICA decomposes the filtered EEG data to identify and separate the independent components. After that, the components related to the EEG activity are retained as needed, while the components representing interference are eliminated for the purpose of removing artifacts. Finally, the EEG signals were downsampled to 500Hz and A1 and A2 were selected as the reference electrodes, the invalid electrodes were removed and feature extraction was performed in the range of 60s ~ 120s, with each segment averaged at 2s.

Adjacency matrix

Phase synchronization analysis is an effective method to infer brain function and neural activity based on EEG signals. In this study, we extracted the phase synchronization degree between two EEG signals by calculating the PLI and PLV, and thus constructed the neighboring matrix to build a brain network model, which consists of network nodes and edges between nodes, and there are three steps to build a brain network: ① define the network nodes: electrodes are usually selected as the nodes of the network, and different nodes represent different brain regions. ② Define the edges of the network: the edges of the network are the connectivity between the nodes, representing the connection between different brain regions. The neighbor matrix is obtained by quantifying the relationship between the nodes, and the weights of the edges represent the connections between the brain regions. ③ Selection of threshold value: by selecting a suitable threshold value will be the adjacency matrix, the matrix is the brain network model obtained from the construction, this study by selecting two kinds of coefficients to construct different brain networks for better comparative analysis.

(1) Phase Lag Index (PLI) was used to quantify the functional connectivity between each EEG channel pair with the following equation:

$$PLI = |E[sign(\phi_y(j\Delta t))]|. \tag{1}$$

PLI captures the asymmetry in the distribution of phase difference between two signals and is calculated based on the relative phase difference between the two signals. Where E is the expected value, where i, j are integers, sign is the sign function, ϕx and ϕy are the phases of the two time series x, y. The PLI varies between 0 and 1. When the PLI is 0, there is no phase synchronization of the two time series; when the PLI is 1, the two time series are perfectly synchronized with each other. According to the above equation, a 19×19 PLI function connectivity matrix can be obtained at each time–frequency point.

The neighboring matrix constructed based on the PLI method for the average of the three populations is shown in Fig. 12:

(2) The phase locking value (PLV) phase–amplitude coupling method analyzes the mutual modulation interaction between the signals of each channel [37]. Assuming 2 different signals x(t) and y(t), their corresponding PLVs are shown in equation:

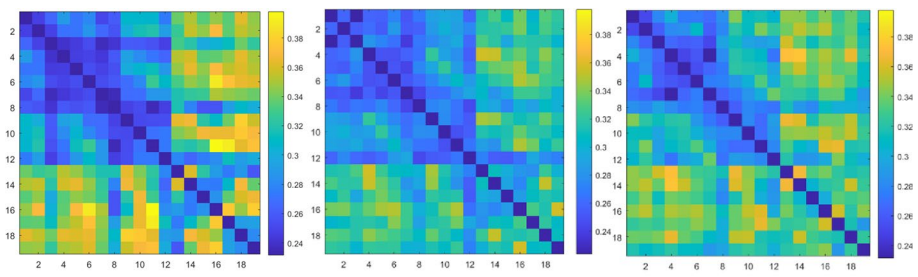

(a)AD (b)MCI (c)HC

Fig. 12 The adjacency matrix of three groups of people is constructed based on PLI method

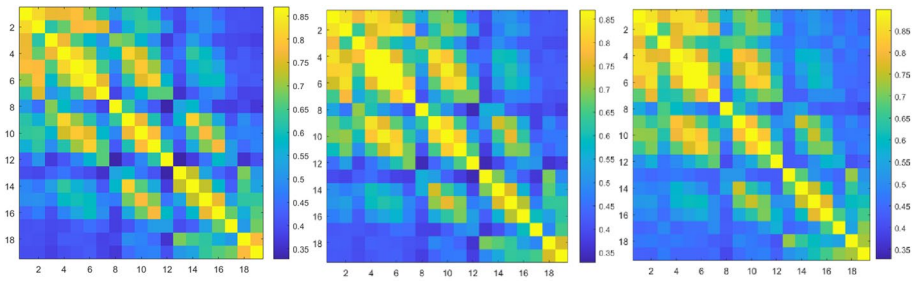

(a)AD (b)MCI (c)HC

Fig. 13 The adjacency matrix of three groups of people is constructed based on PLV method

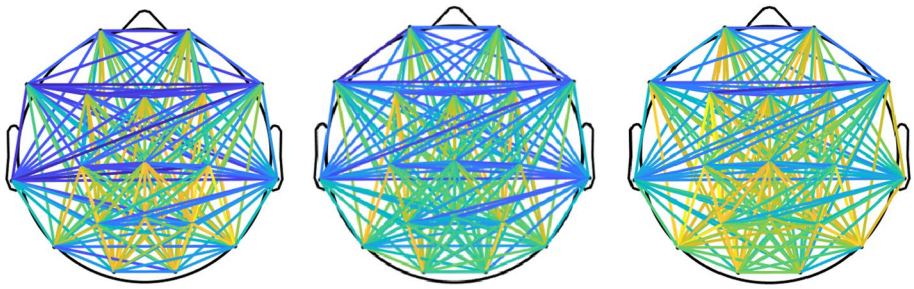

(a)AD (b)MCI (c)HC

Fig. 14 PLI functional connection diagram

$$\begin{aligned} \mathrm{PLV}\left|e_t^{i\phi_{xy}(t)}\right| &= \sqrt{\cos\phi_{xy}(t)_t^2 + \sin\phi_{xy}(t)_t^2} \\ \phi_{xy}(t) &= \phi_x(t) - \phi_y(t), \end{aligned} \tag{2}$$

where i denotes the imaginary unit; ϕxy is the instantaneous phase difference between x (t) and y (t) resolved signals; ϕx (t) and ϕy (t) are the instantaneous phases of x (t) and y (t) resolved signals, respectively. PLV takes the value in the range of [0, 1], and there is no phase synchronization of the two signals when PLV = 0. When PLV = 1, the two signals have a stable phase difference, i.e., they are synchronized with the phase. The neighbor matrix of the three population averages constructed based on the PLV method is shown in Fig. 13.

PLI functional connection analysis

In this study, we extracted the preprocessed EEG after the onset of resting and a frequency range of 8 ~ 13Hz (α band) to obtain the weighted functional adjacency matrix of resting correlation for each subject, as shown in Fig. 12 above. The horizontal and vertical coordinates in the figure are all 19 channels, and the matrix value is the association strength of EEG signals between the corresponding two channels, with lighter colors representing larger values and stronger association strength. The PLI brain functional connectivity map was drawn according to the brain functional neighboring matrix, as shown in Fig. 14. It can be seen that the differences in PLI brain functional connectivity between healthy people and MCI patients are small, while the differences in AD patients

Table 3 Comparison of PLI functional connectivity among three groups of people

Electrodes	AD	MCI	HC	P-value
O1-P3	0.3682 ± 0.009	0.3535 ± 0.012	0.3565 ± 0.019	< 0.01
C4-P4	0.3981 ± 0.010	0.3485 ± 0.015	0.3620 ± 0.022	< 0.01
F3-T5	0.3754 ± 0.007	0.3641 ± 0.011	0.3693 ± 0.018	< 0.01

Table 4 Statistical analysis results under the PLI-19 channel

PLI-19-channel	Test	Variance test	P-value-test	P-value-Var
AD	0.043	0.042	0.009	0.046
MCI	0.068	0.078	0.006	0.033
HC	0.032	0.009	0.005	0.011

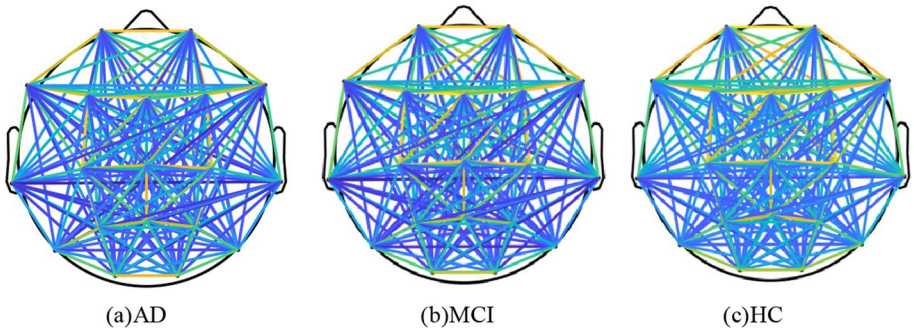

Fig. 15 PLV functional connection diagram

are obviously weaker in the association strength between the channels at the parietal and occipital lobes. Among them, different color bars indicate the connection strength. It can be seen that the brain network established based on PLI has greater differences in AD patients compared to healthy people. Then, the Fisher score was used for analysis, and the first two features with higher scores were selected for comparison [38], as shown in Table 3. Statistical analysis of functional connectivity yielded that all three groups were statistically different, as shown in Table 4. In the PLI's functional connectivity statistical analysis, we extracted the preprocessed EEG, quantified its 19-channel values, and subjected them to independent samples t-test and one-way ANOVA, respectively. The results showed that quantifying the 19-channel values of the three populations, the significance result of the independent samples t-test was P-value < 0.05 due to the fulfilment of variance Chi-square, thus statistically significant, indicating a significant difference in PLI. The ANOVA result of the one-sample ANOVA test was P-value < 0.05 due to the fulfilment of variance Chi-square, thus statistically significant, indicating a significant difference between the different populations.

PLV functional connection analysis

In this study, we extracted the preprocessed EEG after the onset of resting and a frequency range of 8-13Hz (α-band) to obtain the weighted functional adjacency matrix

Table 5 Comparison of PLV functional connectivity among three groups of people

Electrodes	AD	MCI	HC	P-value
C3-C4	0.6078 ± 0.005	0.6493 ± 0.014	0.6721 ± 0.024	< 0.01
FP2-CZ	0.6370 ± 0.007	0.7011 ± 0.018	0.7163 ± 0.020	< 0.01
F4-CZ	0.7547 ± 0.002	0.8088 ± 0.010	0.8209 ± 0.028	< 0.01

Table 6 Statistical analysis results under the PLV-19 channel

PLV-19-channel	Test	Variance test	P-value-test	P-value-Var
AD	0.022	0.045	0.005	0.031
MCI	0.014	0.026	0.006	0.030
HC	0.006	0.012	0.003	0.011

of resting correlation for each subject, as shown in Fig. 13. The horizontal and vertical coordinates in the figure are all 19 channels, and the matrix value is the association strength of EEG signals between the corresponding two channels, with lighter colors representing larger values and stronger association strength. The PLV brain functional connectivity map was drawn according to the brain functional neighboring matrix, as shown in Fig. 15. It can be seen that the differences in PLV brain functional connectivity between AD patients and MCI patients are small, and both are significantly different from HC, mainly concentrated between the frontal and parietal lobes. Among them, different color bars indicate the connection strength. It can be seen that the brain network established based on PLV AD patients have larger differences compared to healthy people. Then, the Fisher score was used for analysis, and the first three features with higher scores were selected for comparison, as shown in Table 5. Statistical analysis of functional connectivity yielded that all three groups were statistically different, as shown in Table 6. In the functional connectivity statistical analysis of PLV, we also extracted the preprocessed EEG, quantified its 19-channel values, and performed independent samples t-test and one-way ANOVA on it, respectively. The results showed that quantifying the 19-channel values of the three populations, the significance result of the independent samples t-test was P-value < 0.05 due to the fulfilment of variance Chi-square, thus statistically significant, indicating that there was a significant difference in PLV. The ANOVA result of the one-way ANOVA test was P-value < 0.05 due to the fulfilment of variance Chi-square, thus statistically significant, indicating that there was a significant difference between the different populations.

Deep learning model

Because of their powerful graph representation, graph neural networks are widely used in various graph tasks, including graph classification [39], prediction [40] and node classification [41], and our brain network analysis deals with node classification. A graph is a complex nonlinear data structure that is generally used to describe the situation where there are one-to-many relationships in the data [42]. In EEG analysis the connection strength between channels is considered to be directionless, so it is generally

represented by an undirected graph G = (V, E), where V = {v_1, v_2, ..., v_n} and E denotes the set of vertices and the set of edges, respectively. In the graph, A is defined as the connection matrix of the graph G. Each element in A corresponds to the case of an edge between two nodes, i.e.:

$$Aij = \exp(xi, xj), \tag{3}$$

where x_i and x_j denote the eigenvectors of nodes v_i and v_j, respectively. After calculating the connection matrix, the corresponding graph Laplacian matrix L can be created:

$$L = D - A, \tag{4}$$

$$Lsym = D^{-1/2}LD^{-1/2} = I - D^{-1/2}AD^{-1/2}, \tag{5}$$

where L_{sym} is the new graph Laplacian matrix after completing the symmetric normalization, and I is the unit matrix. According to the above, referring to the research of Hong et al. [43] and based on the properties of Fourier transform and inverse transform, the calculation method of graph convolution can be written as follows:

$$G[f \otimes g_\theta] = Ug_\theta U^T f. \tag{6}$$

In this study, the GCN model was used to extract the brain network variability of the three populations based on PLI/PLV feature vectors and node features, respectively, for the two phasing methods. Since the convolutional layer of GNN can effectively extract the features from the input data, it has been widely and successfully applied in the fields of signal recognition, natural language processing, etc. Here, in order to study phase synchronization, PLI and PLV features are selected as edges and nodes, respectively. The representation h_v of each node v of the GCN, and the representation of each node is computed from the features x_v of that node, the features $x_{co[v]}$ of the edges connected to that node, and also, the representation $h_{ne[v]}$ of the neighbors of that node, and the features $x_{ne[v]}$ of its neighboring nodes [44]:

$$h_v = f\left(x_{[v']}x_{co[v']}\, h_{ne[v]'}x_{ne[v]}\right). \tag{7}$$

GCN is a kind of the most basic GNN model transformed from the generalized domain [45]. If the graph data has N nodes, and each node has its own features, assuming that the features of these nodes form an N×D dimensional matrix X, and the relationship between each node will also form an N×N dimensional matrix A, also known as the adjacency matrix, at this time X and A are the inputs to the GCN model. Its core formula is as follows:

$$H^{(I+1)} = \sigma\left(\widetilde{\tilde{D}^{-\frac{1}{2}}\tilde{A}\tilde{D}^{-\frac{1}{2}}}H^{(I)}W^{(I)}\right), \tag{8}$$

where I is the unit matrix, $\tilde{D}$ is the degree matrix of $\tilde{A}$, H is the feature of each layer, which for the input layer is X, and σ is the nonlinear activation function ReLU.

Author contributions
Cao Jiayi was responsible for writing the paper, Li Bin was responsible for data collection and Li Xiaoou was responsible for revising and guiding the paper.

Funding
This work was supported in part by Shanghai Municipal Science and Technology Plan Project (22010502400), and Research Project of Yangpu District Technical Committee and Health Commission in Shanghai (YPM202114), and Shanghai University of Medicine & Health Sciences Mental Health Research Institute Foundation (YJYPI202402).

Availability of data and materials
No datasets were generated or analyzed during the current study.

Declarations

Ethics approval and consent to participate
All procedures performed in studies involving human participants were in accordance with the ethical standards of the institutional and/or national research committee. We have obtained the ethical approval for Alzheimer's disease data from Shanghai Yangpu Mental Health Center, Shanghai, China.

Informed consent
Informed consent was obtained from all individual participants included in the study.

Competing interests
The authors declare no competing interests.

Received: 3 June 2024 Accepted: 2 March 2025
Published online: 09 March 2025

References

1. Javaid SF, Giebel C, Khan MAB, et al. Epidemiology of Alzheimer's disease and other dementias: Rising global burden and forecasted trends. F1000Res. 2021;10:425–38.
2. Cahill S. WHO's global action plan on the public health response to dementia: some challenges and opportunities. Aging Ment Health. 2020;24(2):197–9.
3. Zhao L. Alzheimer's disease facts and figures. Alzheimers Dement. 2020;16(3):391–460.
4. Cutler SJ, Brăgaru C. Long-term and short-term predictors of worries about getting Alzheimer's disease. Eur J Ageing. 2015;12:341–51.
5. Kirschstein T, Köhling R. What is the source of the EEG? Clin EEG Neurosci. 2009;40(3):146–9.
6. Kang J, Tian Z, Wei J, et al. Association between obstructive sleep apnea and Alzheimer's disease-related blood and cerebrospinal fluid biomarkers: a meta-analysis. J Clin Neurosci. 2022;102:87–94.
7. Nie J, Zhang Z, Wang B, et al. Different memory patterns of digits: a functional MRI study. J Biomed Sci. 2019;26:1–9.
8. Sun W, Su Y, Wu X, et al. EEG denoising through a wide and deep echo state network optimized by UPSO algorithm. Appl Soft Comput. 2021;105: 107149.
9. Briels CT, Schoonhoven DN, Stam CJ, et al. Reproducibility of EEG functional connectivity in Alzheimer's disease. Alzheimer's research & therapy. 2020;12:1–14.
10. Lynn CW, Bassett DS. The physics of brain network structure, function and control. Nature Reviews Physics. 2019;1(5):318–32.
11. Ismail LE, Karwowski W. A graph theory-based modeling of functional brain connectivity based on eeg: A systematic review in the context of neuroergonomics. IEEE Access. 2020;8:155103–35.
12. Handayani N, Haryanto F, Khotimah SN, et al. Coherence and phase synchrony analyses of EEG signals in Mild Cognitive Impairment (MCI): a study of functional brain connectivity. Polish J Med Phys Eng. 2018;24(1):1–9.
13. Cai L, Wei X, Wang J, et al. Reconstruction of functional brain network in Alzheimer's disease via cross-frequency phase synchronization. Neurocomputing. 2018;314:490–500.
14. Knyazeva MG, Jalili M, Brioschi A, et al. Topography of EEG multivariate phase synchronization in early Alzheimer's disease. Neurobiol Aging. 2010;31(7):1132–44.
15. Babiloni C, Lizio R, Marzano N, et al. Brain neural synchronization and functional coupling in Alzheimer's disease as revealed by resting state EEG rhythms. Int J Psychophysiol. 2016;103:88–102.
16. Zheng H, Xiao H, Zhang Y, et al. Time-Frequency functional connectivity alterations in Alzheimer's disease and frontotemporal dementia: An EEG analysis using machine learning. Clin Neurophysiol. 2024. https://doi.org/10.1016/j.clinph.2024.12.008.
17. Hasoon J, Hamilton CA, Schumacher J, et al. EEG functional connectivity differences predict future conversion to dementia in mild cognitive impairment with Lewy body or Alzheimer disease. Int J Geriatr Psychiatry. 2024;39(9): e6138.
18. Ruiz-Gómez SJ, Hornero R, Poza J, et al. Computational modeling of the effects of EEG volume conduction on functional connectivity metrics. Application to Alzheimer's disease continuum. J Neural Eng. 2019;16(6): 066019.
19. Rasquin SMC, Lodder J, Visser PJ, et al. Predictive accuracy of MCI subtypes for Alzheimer's disease and vascular dementia in subjects with mild cognitive impairment: a 2-year follow-up study. Dement Geriatr Cogn Disord. 2005;19(2–3):113–9.
20. Khazaee A, Ebrahimzadeh A, Babajani-Feremi A, et al. Classification of patients with MCI and AD from healthy controls using directed graph measures of resting-state fMRI. Behav Brain Res. 2017;322:339–50.

21. Parisot S, Ktena SI, Ferrante E, et al. Disease prediction using graph convolutional networks: application to autism spectrum disorder and Alzheimer's disease. Med Image Anal. 2018;48:117–30.
22. Zhang H, Geng X, Wang Y, et al. The significance of EEG alpha oscillation spectral power and beta Oscillation phase synchronization for diagnosing probable Alzheimer disease. Front Aging Neurosci. 2021;13: 631587.
23. Zhou Z, Wang Q, An X, et al. A novel graph neural network method for Alzheimer's disease classification. Comput Biol Med. 2024;180: 108869.
24. Yu WY, Sun TH, Hsu KC, et al. Comparative analysis of machine learning algorithms for Alzheimer's disease classification using EEG signals and genetic information. Comput Biol Med. 2024;176: 108621.
25. Puri DV, Nalbalwar SL, Ingle PP. EEG-based systematic explainable Alzheimer's disease and mild cognitive impairment identification using novel rational dyadic biorthogonal wavelet filter banks. Circuits Syst Signal Process. 2024;43(3):1792–822.
26. Zhang D, Wang Y, Zhou L, et al. Multimodal classification of Alzheimer's disease and mild cognitive impairment. Neuroimage. 2011;55(3):856–67.
27. Xia W, Zhang R, Zhang X, et al. A novel method for diagnosing Alzheimer's disease using deep pyramid CNN based on EEG signals. Heliyon. 2023. https://doi.org/10.1016/j.heliyon.2023.e14858.
28. Contreras JA, Goñi J, Risacher SL, et al. Cognitive complaints in older adults at risk for Alzheimer's disease are associated with altered resting-state networks. Alzheimer's Dementia. 2017;6:40–9.
29. Wang C, Wang Z, Shi X, et al. Binaural processing deficit and cognitive impairment in Alzheimer's disease. Alzheimers Dement. 2022;18(6):1085–99.
30. Veitch DP, Weiner MW, Aisen PS, et al. Using the Alzheimer's disease neuroimaging initiative to improve early detection, diagnosis, and treatment of Alzheimer's disease. Alzheimers Dement. 2022;18(4):824–57.
31. Lin P, Zhu G, Xu X, et al. Brain network analysis of working memory in schizophrenia based on multi graph attention network. Brain Res. 2024. https://doi.org/10.1016/j.brainres.2024.148816.
32. Alves CL, Pineda AM, Roster K, et al. EEG functional connectivity and deep learning for automatic diagnosis of brain disorders: Alzheimer's disease and schizophrenia. J Phys. 2022;3(2): 025001.
33. Rad EM, Azarnoosh M, Ghoshuni M, et al. Diagnosis of mild Alzheimer's disease by EEG and ERP signals using linear and nonlinear classifiers. Biomed Signal Process Control. 2021;70: 103049.
34. Ieracitano C, Mammone N, Bramanti A, et al. A convolutional neural network approach for classification of dementia stages based on 2D-spectral representation of EEG recordings. Neurocomputing. 2019;323:96–107.
35. Kramer MA, Chang FL, Cohen ME, et al. Synchronization measures of the scalp electroencephalogram can discriminate healthy from Alzheimer's subjects. Int J Neural Syst. 2007;17(02):61–9.
36. Akrami A, Solhjoo S, Motie-Nasrabadi A, et al. EEG-based mental task classification: linear and nonlinear classification of movement imagery[C]//2005 IEEE Engineering in Medicine and Biology 27th Annual Conference. IEEE, 2006: 4626–4629
37. Fiscon G, Weitschek E, Felici G, et al. Alzheimer's disease patients classification through EEG signals processing[C]//2014 IEEE Symposium on Computational Intelligence and Data Mining (CIDM). IEEE, 2014: 105–112.
38. Bo D, Wang X, Shi C, et al. Beyond low-frequency information in graph convolutional networks. Proceedings of the AAAI conference on artificial intelligence. 2021; 35(5): 3950–3957
39. Bagherzadeh S, Maghooli K, Shalbaf A, et al. Emotion recognition using effective connectivity and pre-trained convolutional neural networks in EEG signals. Cogn Neurodyn. 2022;16(5):1087–106.
40. Zhang M, Cui Z, Neumann M, et al. An end-to-end deep learning architecture for graph classification. Proceedings of the AAAI conference on artificial intelligence. 2018, 32(1).
41. Schlichtkrull M, Kipf TN, Bloem P, et al. Modeling relational data with graph convolutional networks. Cham: Springer International Publishing; 2018.
42. Li Y. A survey of EEG analysis based on graph neural network[C]//2021 2nd International Conference on Electronics, Communications and Information Technology (CECIT). IEEE, 2021: 151–155.
43. Hong D, Gao L, Yao J, et al. Graph convolutional networks for hyperspectral image classification. IEEE Trans Geosci Remote Sens. 2020;59(7):5966–78.
44. Klepl D, He F, Wu M, et al. EEG-based graph neural network classification of Alzheimer's disease: an empirical evaluation of functional connectivity methods. IEEE Trans Neural Syst Rehabil Eng. 2022;30:2651–60.
45. Klepl D, Wu M, He F. Graph neural network-based eeg classification: a survey. IEEE Trans Neural Syst Rehabil Eng. 2024. https://doi.org/10.1109/TNSRE.2024.3355750.

Publisher's Note